Structure and Luminescence Properties of Poly(1-hexyl-3,4-dimethyl-2,5-pyrrolylene)

Jun-Gill Kang,* Tack-Jin Kim, Changmoon Park,* Lee Sang Woo,‡ and In Tae Kim†

Department of Chemistry, Chungnam National University, Daejeon 305-764, Korea
‡Department of Chemistry, Kwangwoon University, Seoul 139-701, Korea
Received February 13, 2004

A poly(1-hexyl-3,4-dimethyl-2,5-pyrrolylene) (PHDP) was prepared and its luminescence in tetrahydrofuran (THF) was studied. When PHDP is excited by UV light, it produces very strong blue luminescence. The quantum yield of PHDP (Q = 36.9%) is much greater than that of the monomer, 1-hexyl-3,4-dimethylpyrrole (HDP) with Q = 0.61%. The principal luminescence of PHDP has a single decay component with *ca.* 1 ns, whereas the decay of HDP is complicated. The molecular structure and conformational behavior of HDP and the oligomers up to trimer have been also determined by *ab initio* Hartree-Fock (HF/6-31G**), density functional theory (DFT-B3LYP/6-31G**), and semiempirical (ZINDO) methods. According to the results of calculations, it is proposed that the enhanced quantum yield of the polymer PHDP results mostly from the π-conjugation between neighboring pyrrole rings.

Key Words : Poly(1-hexyl-3,4-dimethyl-2,5-pyrrolylene), Luminescence, Quantum yield, Structural calculation

Introduction

Semiconducting and conjugated polymers have attracted great interest due to their applications to light-emitting diodes (LEDs).[1] Poly(*p*-phenylenevinylene) and their derivatives are typical compounds which have been extensively investigated and developed for LEDs.[2] Although there has been great effort to improve their thermal stability, solubility in conventional organic solvents and high luminescence efficiency, most of soluble conjugated polymers have difficulties with color tunability in violet-blue region. Conducting polypyrroles have also shown tremendous technological potentials and can be incorporated in electro-optical devices including molecular electronic devices,[3] electrolytic capacitors,[4] actuators[5] and sensors.[6] However, the optical properties of substituted polypyrroles, such as luminescence and excitation spectra, decay time and quantum efficiency, have not been reported yet, perhaps due to their weak luminosity.

Previously, substituted polypyrrole derivatives, such as poly(1-hexyl-2,5-pyrrolylene) (PHP) and poly(1-hexyl-2,5-pyrrolylene vinylene) (PHPV) were synthesized.[7] Their conductivities were found to be 1.2×10^{-6} and 2.5 S cm^{-1}, respectively. The striking difference in the conductivity between them could be due to steric interactions between adjacent rings. Recently, using a new preparative route to 1-hexyl-3,4-dimethylpyrrole (HDP), we successfully synthesized poly(1-hexyl-3,4-dimethyl-2,5-pyrrolylene) (PHDP), a soluble conducting compound.[8] Of interest, PHDP excited by UV light produces very bright blue emission, which is promising for applications in blue luminescence devices. In this study, we obtained excitation and luminescence spectra and determined the decay lifetime and quantum efficiency. We also performed *ab initio* and semiempirical calculations for the monomer (HDP) and its oligomers to interpret the observed optical properties of PHDP. The theoretical calculations for oligopyrroles provide useful information about the electronic and optical properties of their polymers.[9] The geometries of monomer, dimer, and trimer were optimized, and torsional potentials of trimer were calculated as a model of the PHDP chain on the level of both HF/6-31G** and DFT-B3LYP/6-31G** using Jaguar quantum mechanical program.[10] With the quantum mechanically optimized geometries of monomer, dimer, and trimer, the ZINDO semiempirical method from Gaussian 98[11] was used to study the electronic structures of the oligomers. The experimentally observed luminescence properties of both HDP and PHDP are discussed using the results of theoretical calculations on the modeled structures.

*To whom correspondence should be addressed: Jun-Gill Kang (jgkang@cnu.ac.kr), Changmoon Park (parkcm@cnu.ac.kr)

Experimental Section

Synthesis. As shown in Scheme 1,[8] *cis*-2,3-dimethyl-2-butene-1,4-diol (**2**) was formed by the reduction of dimethylmaleic anhydride (**1**) with $LiAlH_4$ under reflux. The bromination of 2 with PBr_3 (Et_2O, at 0 °C for 1 h, r.t. for 24 h) generated *cis*-1,4-dibromo-2,3-dimethyl-2-butene (**3**). Bromide 3 reacted with three equivalents of hexylamine (benzene, at 0 °C for 1 h, r.t. for 7 days) to yield a cyclic product, 1-hexyl-3,4-dimethyl-3-pyrroline (**4**), which was a valuable intermediate for the synthesis of 1-alkylsubstituted-3,4-dimethylpyrroles. Oxidation of cyclic product 4 with 30% hydrogen peroxide for 12 h at room temperature, followed by direct reaction with acetic anhydride at 0 °C for 12 h gives a 57% yield of 1-hexyl-3,4-dimethylpyrrole (**5**). This monomer 5 was smoothly polymerized by iron chloride (III) hexahydrate and gave poly(1-hexyl-3,4-dimethylpyrrole) (**6**). The resulting oxidized polymer was precipitated in ethanol, reduced in $CHCl_3$ solution with concentrated aque-

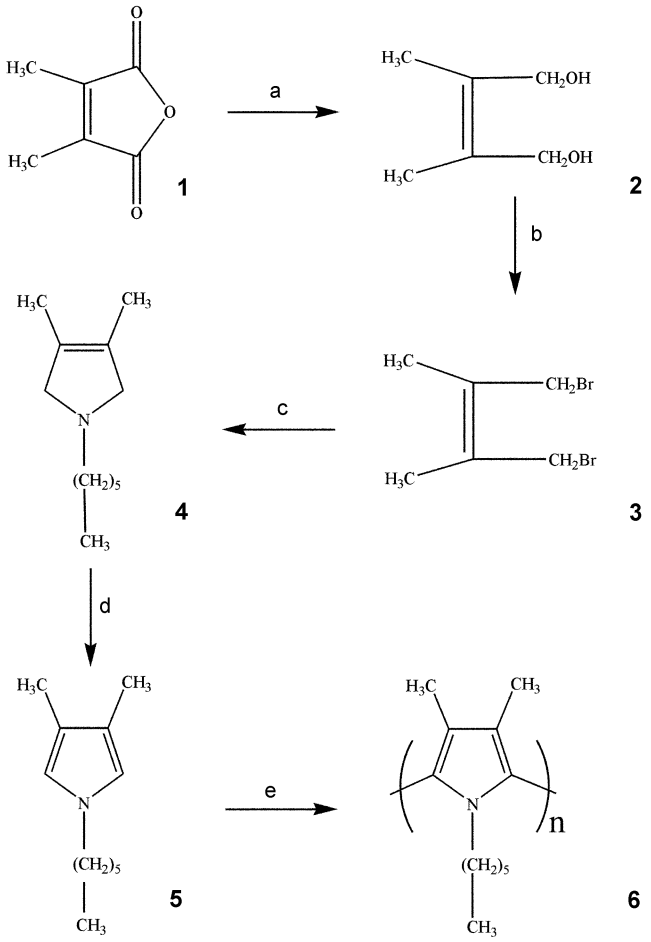

Scheme 1. a) Lithium aluminium hydride, ethyl ether, 12 h, Reflux, 74%; b) Pyridine, PBr_3, r.t. 24 h, 75%; c) Hexylamine, benzene, r.t. 7 days, 38%; d) 30% H_2O_2, r.t. 12 h, acetic anhydride, 0 °C, 12 h, 57%; e) Iron chloride(III) hexahydrate, acetonitrile, 0 °C, 12 h, 30% aqueous ammonium hydroxide, 89%.

ous NH_4OH, and reprecipitated in ethanol to yield a white powder, which was completely soluble in THF, $CHCl_3$, hexane and CH_2Cl_2.

Optical Measurements. The luminescence and excitation spectra were measured at 90° angle with an ARC 0.5 m Czerny-Turner monochromator equipped with a cooled Hamamatsu R-933-14 PM tube. The sample, dissolved in tetrahydrofuran (THF) and deoxygenated with nitrogen gas, was irradiated with a He-Cd 325-nm laser line to obtain the photoluminescence (PL) spectra. To measure excitation spectra, the sample was irradiated with the light from an Oriel 1000 W Xe lamp (working power, 400 W) passing through an Oriel MS257 monochromator. To measure the decay time measurement, we used a time-correlated single photon counting system with an Edinburg FL 900 spectrophotometer.

Quantum yield was measured with a custom-built integrating sphere, manufactured by Lapshere. The 10 cm diameter sphere is hollow and coated on the inside with diffusely reflecting materials. A laser beam was near-normally directed into the sample surface or the inside wall of the sphere through a small entrance hole at the equator of the sphere, but the reflected beam was not allowed to escape through the entrance hole. A diffusely reflecting baffle was positioned between the sample and the exit port in order to protect against direct illumination. The output of the sphere was directed into an ARC 0.5 m Czerny-Turner monochromator equipped with a cooled Hamamatsu R-933-14 PM tube.

Three measurements were made to evaluate an absolute quantum yield, Q, defined by:

$$Q = \frac{\text{number of photons emitted}}{\text{number of photos absorbed}}$$

First, we measured the spectrum of a quartz cuvet filled with solvent only within the sphere. Then, we measured the spectrum of a dissolved sample placed in the sphere when the excitation beam hit the sphere wall. The third measurement was similar to the second, except that the excitation beam hit the sample directly. The spectral areas over the respective excitation and emission wavelength regions, L and P, are proportional to the numbers of excitation and emitted photons, respectively. We calculated the absorption coefficient, A, defined as

$$A = \left(1 - \frac{L_c}{L_b}\right)$$

where L_b and L_c are the spectral areas for the second and third measurements, respectively. The number of absorbed photons is proportional to A times the spectral area of the first measurement, L_a. Correcting for the emission induced indirectly from the reflected excitation beam, the quantum yield can be expressed by[12a]

$$Q = \frac{P_c - (1 - A)P_b}{L_a A}$$

where P_b and P_c are the spectral areas under the emission profiles for the second and third measurements, respectively.

Experimental error in the quantum yield may originate from the degradation of the material during the excitation. To avoid the degradation, the laser beam intensity is deduced by passing it through a water filter. Further error may also originate from the uncertainty in the spectral response of the integrating sphere and the optical system. A calibrated Oriel 45 W Quartz Tungsten Halogen lamp standard was used to measure the spectral response of the integrating sphere and the optical system as one system. To minimize errors due to these imperfections the measurements are repeated several times. The system was also tested by BAM:Eu^{2+} with a high quantum yield.[12b]

Results and Discussion

PL and Excitation Spectra. The photoluminescence (PL) and the excitation spectra of PHDP and the monomer dissolved in THF were measured at room temperature. As shown in Figure 1, both produce blue luminescence. The polymer produces strongly enhanced luminescence spec-

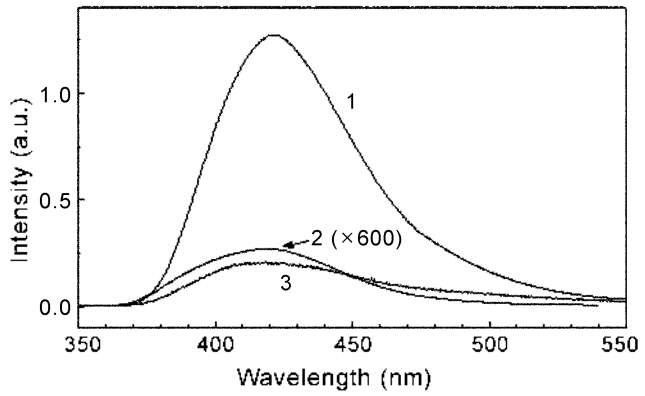

Figure 1. PL spectra of PHDP (1), HDP (2) and PVK (3) dissolved in THF (0.28 wt.%, λ_{exc} = 325 nm).

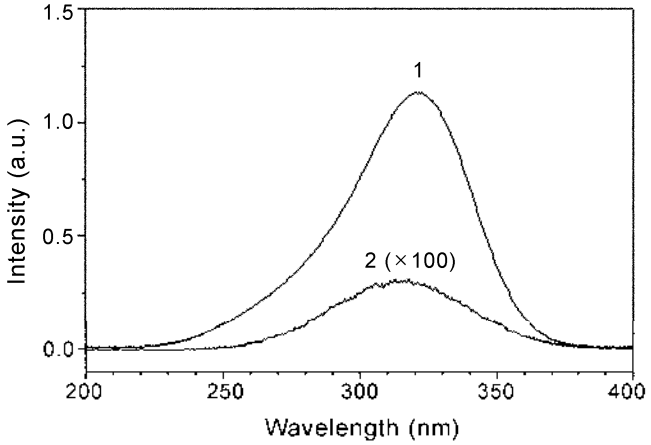

Figure 2. Excitation spectra of the emissions from PHDP(1) and HDP(2) dissolved in THF (0.28 wt%, λ_{ems} = 420 nm).

trum in the 350-550 nm, compared with the case of the monomer. The peak position of the luminescence of the polymer is slightly red-shifted to 423 nm, with respect to that of the monomer (415 nm). This is very unusual, since conjugated polymers usually produce a large red shift in their absorption and luminescence spectra, compared with the respective monomers. The most striking feature, however, is the relative intensity between the polymer and monomer. The luminescence intensity of the polymer is markedly enhanced, compared with that of the monomer. The full width at half maximum (FWHM) of the PHDP luminescence band is much narrower than that of the monomer; FWHM is 3420 cm^{-1} for PHDP *vs.* 4080 cm^{-1} for the monomer. The resolution of the spectrum was performed by using the Gaussian formula. The PL band of PHDP resolved into two components, peaking at 23900(±20) cm^{-1} (418.4 nm) as a main component and 22000(=240) cm^{-1} (454.5 nm) as a low-energy shoulder. The PL band of the monomer consists of two components, peaking at 24100(±80) cm^{-1} (414.9 nm) as a main component and 21760(±260) cm^{-1} (459.6 nm) as an intermediate one accompanying a broad and weak component as a low-energy shoulder. The position of the main component of the polymer are slightly red-shifted by *ca.* 200 cm^{-1}, with respect to that of the monomer. The luminescence of PHDP is very comparable with that of poly(N-vinylcarbazole) (PVK), which is widely used as a sensitizer[13] and emitter.[14,15] Like PHDP, PVK in THF excited at UV wavelengths produces blue emission in the 360-500 nm region, as shown in Figure 1.

Figure 2 shows the excitation spectra of the 420-nm emissions from the monomer and polymer. As expected, the shape of the spectrum of the polymer is very similar to that of the monomer, although the excitation spectrum of the polymer is much more intense than that of the monomer. Both bands are asymmetric, which resolved into 30990(±12) cm^{-1} (322.7 nm) as a main component and 34470(=170) cm^{-1} (290.1 nm) as an additional component for the polymer, and 31400(±70) cm^{-1} (318.5 nm) as a main and 34700 (=300) cm^{-1} (288.2 nm) as an additional for the monomer.

Structural Calculations. To understand the observed luminescence properties, the geometries of monomer, dimer and trimer were optimized at the levels of both HF/6-31G** and DFT-B3LYP/6-31G** using the Jaguar quantum mechanical program.[10] The optimized structure of the monomer was found to belong to group C_s in which the pyrrole ring and the first carbon of the hexyl group attached to the nitrogen of the pyrrole ring are nearly in plane, with the hexyl group in its extended conformation. As shown in Figure 3, there are three low-energy conformations for the dimer. Of these, the dimer-*a* conformation with C_2 symmetry turned out to be the lowest energy structure. In the dimer-*a* conformation, the pyrrole rings of the neighboring monomers are twisted at an angle of about 70°, as indicated by the torsion angle of N1-C2-C2'-N1' (see Figure 4) for both the HF and DFT cases. This large twist results from steric hindrances involving bulky functional groups attached to the backbone: one hexyl and two methyl groups for each monomer unit. For unsubstituted 2,2'-bipyrrole, the two rings are slightly twisted from syn-gauche configuration.[9a] The results of calculations show that there are minor changes in the structure of the monomer unit, whether it exist as a monomer itself or is placed within a dimer or a trimer. This implies that this trend is retained in the polymer. The energies of the two local minimum structures are 0.33-0.53 kcal/mol higher for the case of DFT versus the global minimum structure, while they are 0.69-1.44 kcal/mol higher for the HF case. With these small energy differences, it seems plausible that all three structures in Figure 3 are possible during the process of the dimer formation.

Figure 3 shows three conformations for the trimer, taken into account as the low energy structure. The calculations show that the trimer-*a* structure has the lowest energy, and the other two structures have energies 1.19-1.37 kcal/mol higher for DFT and 1.87-3.13 kcal/mol higher for HF. Compared to the smaller energy differences between dimers, 0.33-0.53 kcal/mol for DFT and 0.69-1.44 kcal/mol for HF, the much larger energy differences between the trimers are big enough to control the orientation of the next monomer being attached to the given dimer, fixing the rotational angle for consecutive monomers throughout the process of poly-

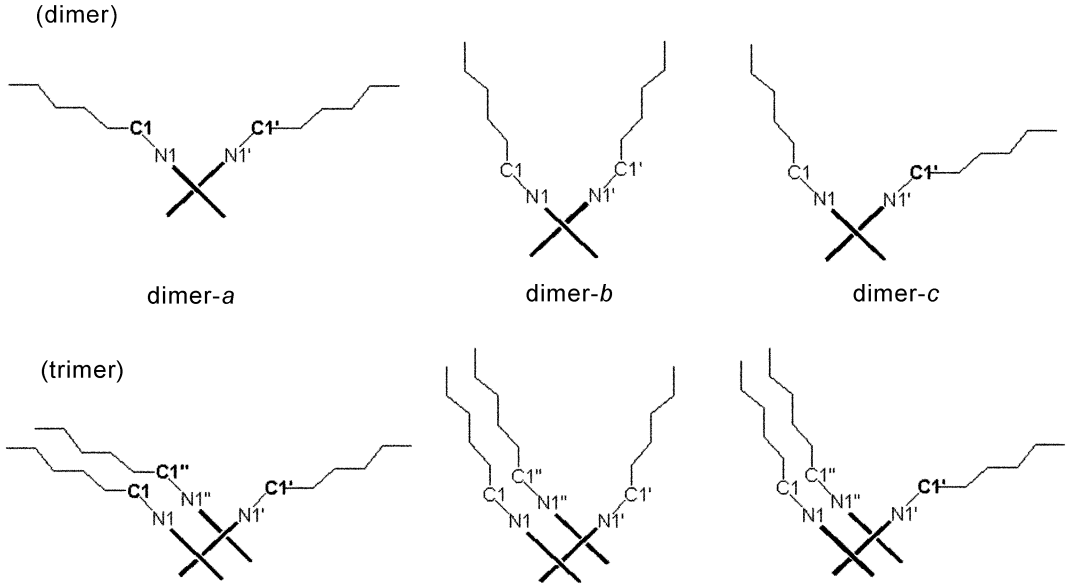

Figure 3. The three low-energy conformations of the dimer and trimer tested to determine the global minimum structure. The bold line represents 2,3-dimethylpyrrole ring.

merization.

To study the rigidity of the structure, the rotational energy barrier between the center and two other neighboring monomers forming the trimer was calculated using the global minimum structure of trimer-*a*. All the geometries were optimized at each fixed torsion angels for both of N1-C2-C2'-N1' and N1'-C5'-C5"-N1" (see Figure 4). As shown in Figure 5, at a torsion angle of 100° (or 50°), the rotational energy barrier is 3.06 (or 3.14) kcal mol^{-1} for HF and 1.85 (or 2.27) kcal mol^{-1} for DFT. The results show that the rotational energy barrier for a trimer is high enough to prevent the constituent monomers from changing their respective torsional angle and to keep a trimer at near their optimum conformation. In a trimer, the two outer monomers interact only with the center monomer. However, in PHDP, every monomer has interactions with two neighboring monomers, making the monomers in a polymer more restricted than those in a trimer. Therefore, in the polymer, the whole structure is predicted to be much more rigid compared to the structure of a trimer at room temperature.

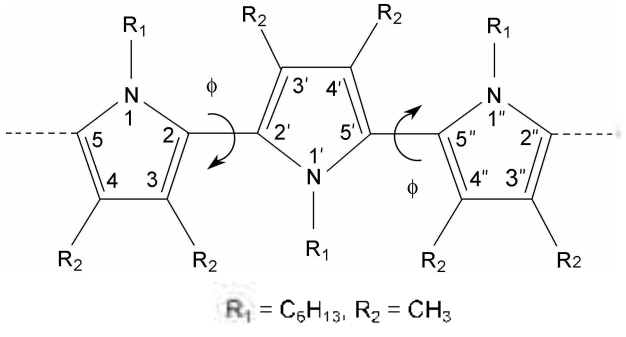

Figure 4. Atom numbers and torsion angle, ϕ, formed by the two backbone rings: $\phi = 0$ for the syn-gauche and $\phi = 180$ for the anti-gauche form.

Using the ZINDO semiempirical method, we calculated the excitation energies and oscillator strengths (f) for the optimized monomer, dimer-*a*, and trimer-*a*. The results for some low-lying excited states are listed in Table 1. For the monomer, the first two lowest excited sates are the ^{1}A' and ^{1}A" states with $f = 0.04$ and 0.22, respectively. As the oligomer extends from monomer to dimer and to trimer, the energy of these two states decreases and the oscillator strength increases. Furthermore, for the oligomer, the energy levels of these two states are reversed. Although the calculated energy-shift is larger than the observed one, these

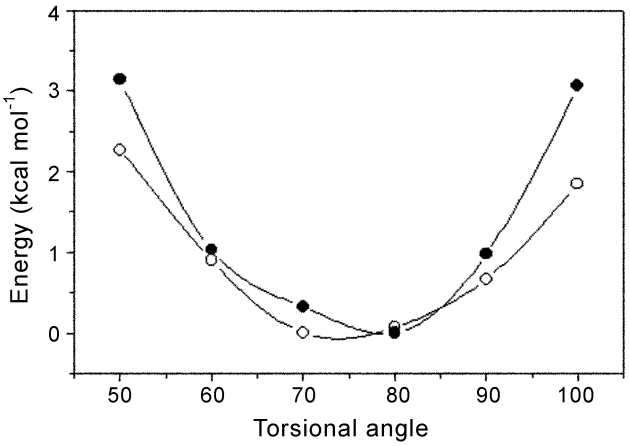

Figure 5. Rotational energy barrier between the center and two neighboring backbones in the trimer. Each point for the relative torsional angle ϕ indicates the relative potential energy for the optimized trimer-*a* at each fixed angle ϕ for both torsional angles of N1-C1-C2-N1' and -ϕ for N1'-C4'-C4"-N1", resulting in C_s symmetry. The lowest energy of trimer-*a* in its C_s symmetry is 0.43 kcal/mol less stable than the global minimum structure of trimer-a. Solid and open symbols represent the optimized values, using HF/6-31G** and DFT-B3LYP/6-31G** methods, respectively.

Table 1. Energies and oscillator strengths for the excited states of the optimized monomer, dimer-*a*, and trimer-*a* (see Figure 3)

monomer			dimmer			trimer[a]		
level	Energy (eV)	f	level	Energy (eV)	f	level	Energy (eV)	f
^{1}A'	5.21	0.04	^{1}B	4.85	0.39	A"	4.52	0.59
^{1}A"	5.47	0.22	^{1}B.	5.14	0.07	A'	4.91	0.05
^{1}A'	5.99	0	^{1}A	5.14	0.01	A"	5.08	0.01
^{1}A"	6.13	0	^{1}A	5.22	0.01	A'	5.12	0.03
^{1}A"	6.65	0.20	^{1}B	5.49	0.01	A"	5.13	0.03
^{1}A"	6.70	0	^{1}A	5.54	0.07	A'	5.13	0.06
^{1}A'	6.83	0	^{1}B	5.55	0.13	A'	5.26	0.07
^{1}A'	6.95	0	^{1}A	5.82	0	A"	5.50	0.05
^{1}A"	7.53	0	^{1}B	6.19	0.01	A'	5.52	0.02
^{1}A'	7.86		^{1}A	6.22	0.03	A"	5.53	0.09
			^{1}B	6.46	0.06	A'	5.60	0.04
			^{1}A	6.49	0	A'	5.65	0.10
			^{1}B	6.65	0.17	A'	6.08	0.04
			^{1}A	6.65	0.08	A"	6.12	0.02
			^{1}B	6.69	0.61	A'	6.41	0.18
			^{1}B	6.72	0.11	A"	6.45	0.01
			^{1}A	6.74		A'	6.47	0.07
			^{1}A	6.83	0.16	A"	6.48	0.01
			^{1}B	7.03	0.15	A'	6.57	0.37
			^{1}A	7.04		A"	6.65	0.10

[a]The optimized structure of trimer-*a* with C_s symmetry as in Figure 3 is used in the calculation.

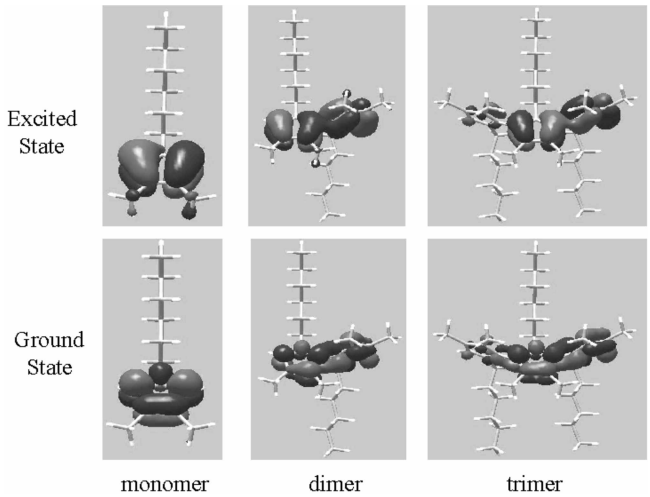

Figure 6. The electronic structures of the ground and excited states responsible for the lowest energy transition for each of monomer, dimer, or trimer.

two excited states are well matched with the experimental results. The main excitation component can be attributed to the transition from the ground state to the first excited ^{1}A" state and the additional band to the transition from the ground state to the first excited ^{1}A" state. Figure 6 shows the molecular orbital (MO) of the first excited ^{1}A" state. According to the results of geometry optimization, the neighboring pyrrole rings are at a torsional angle of around 70 degrees each other, either in a dimer or in a trimer. Nevertheless, the

Table 2. PL quantum yield, Q(%) and decay times of HDP, PHDP and PVK dissolved in THF (0.28 wt.%)

sample	Q (%)	λ_{ems} (nm)	τ_1 (ns)	a_1	τ_2 (ns)	a_2	τ_3 (ns)	a_3
HDP	0.61	400	0.75	0.15	4.73	0.62	14.08	0.23
		420	0.80	0.26	3.28	0.41	8.91	0.33
		500	0.80	0.26	3.25	0.40	8.81	0.34
PHDP	36.9	390	1.03	1.00				
		420	1.06	1.00				
		460	1.09	0.94	3.67	0.06		
		500	1.26	0.77	3.99	0.23		
		520	1.26	0.69	4.12	0.31		
PVK	14.6	390	1.67	0.98	13.4	0.02		
		420	2.7	0.05	16.1	0.95		
		460	15.6	1.00				

MO structures for the dimer and the trimer clearly show that there exist electronic overlaps between neighboring pyrrole rings. The π-conjugation and the rigid conformation are responsible for the luminescence property of the polymer showing the strong luminescence with the narrow FWHM. For the monomer, according to the calculated oscillator strength, the main component can be associated with the ^{1}A" state and the second component with the ^{1}A" state.

Quantum Yields and Lifetimes. The absolute quantum yields of HDP, PHDP and PVK dissolved in THF were measured at room temperature. As listed in Table 2, the luminescence of PHDP with Q = 36.9% was much greater than that of the monomer, HDP, with Q = 0.61%. In general, the quantum yield of the polymer in a good solvent is lower than the case in a solvent with low solubility.[16-18] Moreover, the quantum efficiency of PHDP is 2.5 times as strong as that of the high-efficient conjugated PVK. The high quantum yield of PHDP, which has good solubility in THF, shows the fact that the electronic overlaps between neighboring pyrrole rings can be extended upon the polymerization although there are the large twisted optimum torsional angle of around 70 degrees between the backbones.

The luminescence decay curves of HDP, PHDP and PVK dissolved in THF were measured at room temperature. Figure 7 shows typical observed decays. A log plot of the luminescence data *vs.* times is very useful for identifying whether the decay involves a single component. The decay curve for the monomer, HDP, satisfied the following equation:

$$I(t) = A\exp(-t/\tau_1) + B\exp(-t/\tau_2) + C\exp(-t/\tau_3)$$

where the lifetimes τ_1, τ_2, and τ_3 are derived from the simulation. As listed in Table 2, the values and the weights of the three components for the monomer, HDP, are not very dependent the luminescence wavelength. The multi-exponential decay may be due to inhomogeneities with different conformations, the complicity of the emitting states or the relaxation between the monomer and the solvent. By contrast, for the polymer, PHDP, the number of the decay components is dependent on the luminescence wavelength. At the high-energy side and the peak position, an identical

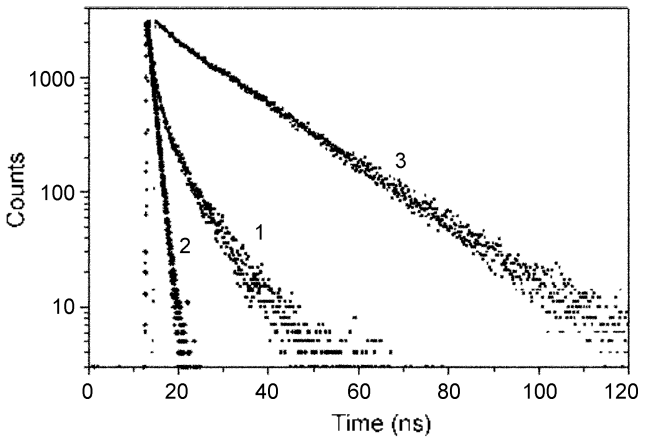

Figure 7. Typical decay-time data for the emissions from HDP (1), PHDP (2) and PVK (3) dissolved in THF (0.28 wt.%).

single component of *ca.* 1.0 ns was found. At the 460-nm emission, there are two components: 1.09 and 3.67 ns. However, the 460-nm emission mainly results from the fast decay component. The contribution of the slow component is only 6%. With increasing the wavelength, the contribution of the slow component increases slightly. At the low-energy shoulder, the contribution of the slow component increases to 31%, but it is lower than that of the fast component. It can be concluded that for PDHP the conformational in homogeneity and the interaction with the solvent could be minor. These results lead us to assign the main 420 nm emission component with *ca.* 1 ns as the transition from the ^{1}A" state to the ^{1}A' ground state and the additional 458 nm component with ca. 4 ns as the $^1A' \rightarrow {}^1A'$ transition. For the monomer, HDP, there might be three segments, responsible for the three lifetime components. The slowest one, which was not observed in the polymer, may be attributed to the relaxation between the monomer and solvent. As seen in the lifetime of the polymer, each emission component has only a single component, so that relaxation between the polymer and solvent can be ruled out.

For PVK, the decay curve of the high-energy emission resolved into two components, 1.67 and 13.4 ns. However, the contribution of the slow component is almost negligible. As the emission wavelength increases, the contribution of the slow component increased markedly and become the major component (95%) at the peak position. Noted that at the low-energy side, the emission has a rising component in the early stage in the decay region. The complexity of the decay of the PVK emission could be related with the conformational inhomogeneities related with the excimer configuration and the aggregation states.[14] The phosphorescence with the long lifetime was not found in the low-energy side emission from all compounds investigated in this study.

Conclusion

The polymer, PHDP, produces much higher luminescence intensity than the monomer does. The theoretical calculations for oligopyrroles show that there exist electronic overlaps between the π electrons of one backbone ring and the π electrons on the neighboring rings, although there is the large torsion-angle between the neighboring backbone planes. The extension of the π electronic overlap in both the ground and excited states may result in the strong emission from the polymer. Due to the large torsion-angle, PDHP forms the highly ordered configuration, *i.e.*, the planes of alternative backbone units are almost parallel and the distance between a N atom and its next-nearest neighbor N atom is as short as 6 Å. The achievement of a higher degree of structural order will additionally enhance the probability of radiative transitions by suppressing the multiphonon nonradiative channel. In contrast with the case of the monomer, the relaxation between the molecule and the solvent was not found in the decay time of the luminescence of the polymer.

Acknowledgment. This work was funded by the Korean Science and Engineering Foundation (KOSEF R01-2001-00055). I. T. Kim and S. W. Lee acknowledge financial support from the Kwangwoon University (2003).

References

1. (a) Burroughes, J. H.; Bradley, D. D. C.; Brown, A. R.; Marks, R. N.; Mackay, K.; Friend, R. H.; Burns, P. L.; Holmes, A. B. *Nature* (London) **1990**, *347*, 539. (b) Gao, J.; Heeger, A. J.; Lee, J. Y.; Kim, C. Y. *Synth. Met.* **1996**, *82*, 221. (c) An, B.-K.; Kim, Y.-H.; Shin, D.-C.; Park, S. Y.; Yu, H.-S.; Kwon, S.-K. *Macromol.* **2001**, *34*, 3993.
2. (a) Clery, D. *Science* **1994**, *263*, 1700. (b) Zheng, M.; Bai, F.; Li, Y.; Yu, G.; Yang, C.; Zhu, D. *Synth. Met.* **1999**, *102*, 1275. (c) Lee, D. W.; Kwon, K.-Y.; Jin, J.-I.; Park, Y.; Kim, Y.-R.; Hwang, I.-W. *Chem. Mater.* **2001**, *13*, 565.
3. Kittlesen, G. P.; White, H. S.; Wrighton, M. S. *J. Am. Chem. Soc.* **1984**, *106*, 7389.
4. (a) Kudoh, Y.; Tsuchiya, S.; Kojima, T.; Fukuyama, M.; Yoshimura, S. *Synth. Met.* **1991**, *41-43*, 1133. (b) Krings, L. H. M.; Havinga, E. E.; Donkers, J. J. T. M.; Vork, F. T. A. *Synth. Met.* **1993**, *54*, 453.
5. Smela, E.; Inganas, O.; Lundstrom, I. *Science* **1995**, *268*, 1735.
6. (a) Kunugi, Y.; Nigorikawa, K.; Harima, Y.; Yamashita, K. *Chem. Commun.* **1994**, 873. (b) Charlestworth, J. M.; Partridge, A. C.; Carrard, N. *J. Phys. Chem.* **1993**, *97*, 5418.
7. (a) Kim, I. T.; Elsenbaumer, R. L. *Chem. Commun.* **1998**, 327. (b) Kim, I. T.; Elsenbaumer, R. L. *Macromol.* **2000**, *33*, 6407.
8. Kim, I. T.; Lee, S. W.; Kwak, T. H.; Lee, J. Y.; Park, H. S.; Kim, S. Y.; Lee, C. M.; Jung, H. E.; Kang, J.-G.; Kim, T.-J.; Kang, H.-J.; Park, C. *Macrol. Rapid Commun.* **2002**, *23*, 551.
9. (a) Brocks, G.; Kelly, P. J.; Car, R. *Synth. Mat.* **1993**, *57*, 4243. (b) Millefiopi, S.; Alparone, A. *J. Chem. Soc. Faraday Trans.* **1998**, *94*, 25. (c) Brocks, G.; Tol, A. *Synth. Mat.* **1999**, *101*, 516. (d) Choi, J.; Chipara, M.; Xu, B.; Yang, C. S.; Doudin, B.; Dowben, P. A. *Chem. Phys. Lett.* **2001**, *343*, 193.
10. *Jaguar 3.5*; Schrödinger, Inc.; Portland, Oregon, 1998.
11. Frisch, M. J.; Trucks, G. W.; Schlegel, H. B.; Scuseria, G. E.; Robb, M. A.; Cheeseman, J. R.; Zakrzewski, V. G.; Montgomery, J. A. Jr.; Stratmann, R. E.; Burant, J. C.; Dapprich, S.; Millam, J. M.; Daniels, A. D.; Kudin, K. N.; Strain, M. C.; Farkas, O.; Tomasi, J.; Barone, V.; Cossi, M.; Cammi, R.; Mennucci, B.; Pomelli, C.; Adamo, C.; Clifford, S.; Ochterski, J.; Petersson, G. A.; Ayala, P. Y.; Cui, Q.; Morokuma, K.; Malick, D. K.; Rabuck, A. D.; Raghavachari, K.; Foresman, J. B.; Cioslowski, J.; Ortiz, J.

V.; Baboul, A. G.; Stefanov, B. B.; Liu, G.; Liashenko, A.; Piskorz, P.; Komaromi, I.; Gomperts, R.; Martin, R. L.; Fox, D. J.; Keith, T.; Al-Laham, M. A.; Peng, C. Y.; Nanayakkara, A.; Challacombe, M.; Gill, P. M. W.; Johnson, B.; Chen, W.; Wong, M. W.; Andres, J. L.; Gonzalez, C.; Head-Gordon, M.; Replogle, E. S.; Pople, J. A.; *Gaussian 98, Revision A.9*; Gaussian, Inc.: Pittsburgh, PA, 1998.

12. (a) de Mello, J. C.; Wittmann, H. F.; Friend, R. H. *Adv. Mater.* **1997**, *9*, 230. (b) Kim, K.-B.; Kim, Y.-I.; Chun, H.-G.; Cho, T.-Y.; Jung, J.-S.; Kang, J.-G. *Chem. Mater.* **2002**, *14*, 5045.
13. McGehee, M. D.; Bergstedt, T. B.; Zhang, C.; Saab, A. P.; O'Regan, M. B.; Bazan, G. C.; Srdanov, V. I.; Heeger, A. J. *Adv. Mater.* **1999**, *11*, 1349.
14. Johnson, G. E. *J. Chem. Phys.* **1975**, *62*, 4697.
15. Kido, J.; Shionya, H.; Nagai, K. *Appl. Phys. Lett.* **1995**, *67*, 2281.
16. Gettinger, C. L.; Heeger, A. J.; Drake, J. M.; Pine, D. J. J. *Chem. Phys.* **1994**, *101*, 1673.
17. Nguyen, T.-Q.; Doan, V.; Schwartz, B. J. *J. Chem. Phys.* **1999**, *110*, 8.
18. Theander, M.; Svensson, M.; Ruseckas, A.; Zigmantase, D.; Sundström, V.; Andersson, A. R.; Inganäs, O. *Chem. Phys. Lett.* **2001**, *337*, 277.